

New insights into partial oxidation model of magnetites and thermal alteration of magnetic mineralogy of the Chinese loess in air

Qingsong Liu,¹ Subir K. Banerjee,¹ Michael J. Jackson,¹ Chenglong Deng,² Yongxin Pan² and Zhu Rixiang²

¹*Institute for Rock Magnetism, Department of Geology and Geophysics, University of Minnesota, Minneapolis, MN 55455, USA*

²*Palaeomagnetism Lab, Institute of Geology and Geophysics, Chinese Academy of Sciences, Beijing, 100029, China*

Accepted 2004 April 30. Received 2004 April 27; in original form 2004 February 9

SUMMARY

New rock magnetic data including low- and high-temperature thermomagnetic runs and hysteresis loops, as well as X-ray diffraction measurements, are presented from the Chinese loess/palaeosols at JiuZhoutai, on the northwestern margin of the Chinese loess plateau, to provide sound constraints on the partial oxidation model of magnetites and variations in magnetic mineralogy, grain size and oxidation states of loess samples during thermal treatments from room temperature up to 700 °C. The results show that the partially oxidized magnetites in samples are first reduced, probably as a result of the burning of organic matter below 300 °C, and then reoxidized above that. However, even after heating to 700 °C the highly diminished (in size) magnetite core still remains stoichiometric as revealed by the 120 K Verwey transition. We conclude that the diffusion of Fe²⁺ from the magnetite core to the surrounding maghemite rim is confined to the oxidation front (magnetite-core/maghemite-rim boundary), and has less effect on the stoichiometry of the magnetite core. The new results also reveal that the absolute number of superparamagnetic grains (magnetite/maghemite) remains relatively stable during heating. Furthermore, the left-downward shift in the data points of Day plots (mainly between 25 and 150 °C) is caused by a decrease in the oxidation gradient. In contrast, the right-upward (mainly between 500 and 650 °C) shift of the Day plots corresponds to a much higher degree of oxidation, resulting in the increase of a new oxidation gradient between the magnetite core (or the residual maghemite mantle) and the newly developed haematite outer rim, which is transformed from maghemite by heating. These new results place strong constraints on the fidelity of palaeomagnetic results from the Chinese loess constructed by thermal demagnetization, and provide a more accurate interpretation of the Day plot and low-temperature magnetic behaviours for these partially oxidized magnetites. Furthermore, this study provides robust lines of evidence for the core–rim coupling model between different magnetic phases (magnetite, maghemite and haematite).

Key words: Chinese loess, low-temperature oxidation, Jiuzhoutai, magnetic mineralogy, mineral magnetism, temperature oxidation.

1 INTRODUCTION

The thick interbedded Chinese loess/palaeosol sequences record palaeomagnetic and palaeoclimatic information for the past 2.5 Myr (Heller & Liu 1982, 1986; Kukla *et al.* 1988; An 2000; Pan *et al.* 2002). Both palaeomagnetic polarity reversals and palaeoclimatic signals carried by the Chinese loess correlate reasonably with the corresponding marine oxygen isotope records (Heller & Liu 1984, 1986; Kukla *et al.* 1988).

The hallmark loess research of Heller & Liu (1982) re-emphasized accurate magnetostratigraphy in order to date the already observed palaeoclimate proxies (from sedimentology, geochemistry and palaeontology). Considerable effort was spent on

discovering the origin of natural remanent magnetization (NRM) and the best remanence-cleaning techniques to isolate the characteristic remanent magnetization (ChRM) (Heller & Liu 1982, 1984). Then came the dramatic discovery (Kukla *et al.* 1988) that magnetic susceptibility can provide a much higher sensitivity and much more quickly measured palaeoclimatic proxy than other geological observations. This redirected most attention to the measurement of magnetic susceptibility and frequency dependence of susceptibility at multiple sites on the Chinese loess plateau (An *et al.* 1993; Chen *et al.* 1999). Research by Zhou *et al.* (1990) and Maher & Thompson (1995) suggested that the susceptibility enhancement of the palaeosol units is caused by finer-grained pedogenic superparamagnetic (SP, <40 nm) particles, and is directly related to the amount

of palaeorainfall (An *et al.* 1991; Banerjee *et al.* 1993; Heller *et al.* 1993; Maher *et al.* 1994). More recent developments in Chinese loess studies are summarized by Liu & Ding (1998), Porter (2001), Evans & Heller (2001) and Tang *et al.* (2003).

For both palaeoclimatic and palaeomagnetic studies on the Chinese loess/palaeosol sequences, a key issue is to accurately determine the magnetic carriers (mineralogy, grain size and non-stoichiometry) of palaeoclimatic proxies and NRM. Chinese loess mainly contains ferrimagnetic magnetite/maghemite, and antiferromagnetic haematite/goethite (Heller & Liu 1984, 1986; Maher & Thompson 1992; Liu *et al.* 1993). However, most of these previous studies have focused more on differences in magnetic mineralogy and grain sizes between the loess and palaeosol units. Less attention has been paid to systematic changes in non-stoichiometry, especially the degree of oxidation of magnetites in natural samples.

The low-temperature oxidation (LTO) of magnetite to maghemite is ubiquitous in natural rocks and sediments, and subtly but significantly changes the properties of magnetites in samples, in turn influencing both the palaeoclimatic and palaeomagnetic records (van Velzen & Dekkers 1999a,b). The physical and chemical environments in Chinese loess favour LTO processes (Liu *et al.* 2002, 2003a). Thus, the subtle changes in the degree of oxidation of magnetites in the Chinese loess/palaeosol sequences may directly relate to palaeoclimatic conditions. Therefore, knowledge of the effects of LTO on the Chinese loess samples is necessary to correctly retrieve palaeoclimatic and palaeomagnetic information from the loess deposits.

However, it is difficult to accurately determine the degree of LTO of magnetite in natural samples because the products of LTO of initially stoichiometric magnetite may consist of an inner magnetite core covered by a maghemitized rim generally occurring mainly at the crystal surface or in fissures (van Velzen & Zijdeveld 1992, 1995; Cui *et al.* 1994). The partially oxidized magnetites have very different magnetic properties from the homogeneously oxidized magnetite examined in synthetic experiments (e.g. Honig 1995), and may mislead the rock magnetic interpretation (Liu *et al.* 2003a). For example, Liu *et al.* (2003a) observed that the palaeosol samples contain a sharper Verwey transition, whereas loess samples exhibit a much broader Verwey transition, seemingly indicating that the loess samples contain more 'altered magnetite' than the palaeosol. However, this appears to conflict with the X-ray diffraction (XRD)

analysis by Liu *et al.* (2003a) that palaeosols are more oxidized than the loess units. Liu *et al.* (2003a) proposed that the maghemite rim and the stoichiometric core could behave independently in the low-temperature measurements.

This study aims to further test the maghemite-rim/magnetite-core model of partially oxidized magnetite by monitoring the evolution of the magnetic properties of partially oxidized magnetites in the Chinese loess during heating in air. Accurate knowledge of changes in magnetic properties of these partially oxidized magnetites during thermal treatments will improve our understanding of changes in magnetic mineralogy, then place more constraints on interpretation of the thermal demagnetization spectrum of the NRM recorded in the Chinese loess/palaeosol sequences.

2 SAMPLING

The Jiuzhoutai (JZT) profile is located in the northwestern margin of the Chinese loess plateau on the sixth terrace of the Yellow River in Lanzhou City (36° N/103° 50' E) (Chen *et al.* 1999). The mean annual temperature is about 6–7 °C, and the mean annual precipitation is about 300–400 mm. Previous studies show that the palaeosol unit S1 (marine isotope stage (MIS) 5) is between 28.6 and 36 m. Three widely separated subpalaeosol units can be assigned unambiguously as S1S1 (MIS 5a) S1S2 (MIS 5c) and S1S3 (MIS 5e) respectively. Among them, the best developed, S1S3, corresponding to MIS 5e, is characterized by a reddish-brown colour.

To get fresh sample, well-exposed outcrops were cut after removing about 50 cm of surface material to eliminate weathering effects. Bag samples were obtained every 2 cm and were first studied by Chen *et al.* (1999). Then, exactly the same set of bag samples was shipped to the University of Minnesota for detailed palaeomagnetic and rock magnetic studies (Liu *et al.* 2003a,b, 2004).

3 EXPERIMENTS

The low-field magnetic susceptibility (Fig. 1) was measured using a Kappabridge susceptometer (KLY-2 with CS-2 furnace). The preliminary stratigraphic boundaries of the section were determined mainly by the susceptibility, thermoluminescence (TL) age controls and visual observation during the field work (Chen *et al.* 1999).

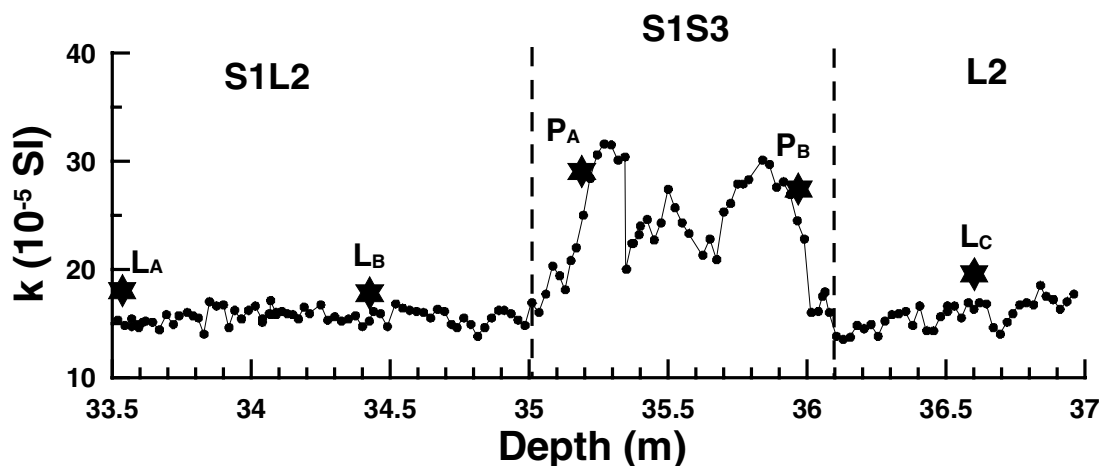


Figure 1. Depth plot of the susceptibility of the JZT section. Dashed lines mark the pedostratigraphic boundaries S1L2/S1S3 and S1S3/L2 respectively. Three representative loess samples (L_A , L_B and L_C) and two palaeosol samples (P_A and P_B) are selected for rock magnetic studies; and further low-temperature experiments are conducted on L_B .

Three characteristic loess samples ($L_A/33.54$ m, $L_B/34.45$ m and $L_C/36.63$ m) and two palaeosol samples ($P_A/35.19$ m and $P_B/35.89$ m) were selected for detailed rock magnetic investigations (Fig. 1). The three loess samples represent the aeolian background with minimum magnetic susceptibility values. In contrast, the two palaeosols with elevated susceptibility values represent the samples with strong pedogenic alterations at this profile.

To determine the possible mineral transformations by heating in air, first, these five samples were heated to 150 and 300 °C and then cooled back to room temperature. The hysteresis loops of the thermal products were measured at room temperature using a Princeton Applied Research vibrating sample magnetometer (VSM2900). Saturation magnetization (M_s), saturation remanence (M_{rs}) and coercivity (B_c) were calculated after subtracting the paramagnetic contribution. The coercivity of remanence (B_{cr}) was determined by the backward DC remagnetization of M_{rs} . A Day plot (Day *et al.* 1977) was constructed to show the systematic changes in the hysteresis properties after heating.

For thermal demagnetization of anhysteretic remanent magnetization (ARM), saturation isothermal remanent magnetization (SIRM) and NRM, fresh samples were progressively thermally demagnetized from room temperature up to 700 °C with steps of 25 °C in air. The samples were held at the elevated temperatures for 30 min, and remanences were measured at room temperature. ARM was imparted in a 200 mT alternating field with a superimposed 50 μ T direct bias field using a Dtech D2000 instrument. M_{rs} and SIRM are used simultaneously in this paper and M_{rs} is specifically referred to the measurements from hysteresis loops.

Frequency-dependent susceptibility was measured using a LakeShore Cryotronics AC susceptometer. The parameter χ_{fd} per cent, is previously expressed as $100 \cdot (\chi_{470 \text{ Hz}} - \chi_{4700 \text{ Hz}}) / \chi_{470 \text{ Hz}}$ computed from dual-frequency measurements on Bartington instruments. However, large uncertainties might arise due to only two endpoint measurements. Therefore, in our study, χ_{fd} per cent was determined more accurately using data acquired at 20 frequencies between 40 and 4000 Hz at room temperature. Linear regression produced excellent fits to the $\chi(\log f)$ data, and best-fit values for 400 and 4000 Hz were used for the subsequent calculations. The absolute difference in susceptibility between 400 and 4000 Hz is defined as $\chi_{fd}(\chi_{400 \text{ Hz}} - \chi_{4000 \text{ Hz}})$.

Thermal demagnetization of the low-temperature saturation isothermal remanent magnetization (LT-SIRM) acquired at 20 K for selected samples was performed with a Quantum Designs magnetic properties measurement system (MPMS). Remanence was measured at temperature increments of 2 K, with an error of ± 0.5 K. To detect the variations in the non-stoichiometry of the magnetic particles in samples, background-corrected first-order derivatives of LT-SIRM were obtained to enhance the behaviour of the Verwey transition (~ 120 K) produced by magnetite (Liu *et al.* 2003b).

To conduct low-temperature cycling (or demagnetization, LTD) of room-temperature remanences, the initial remanence was cooled down from 300 K to 20 K and warmed back to 300 K with a temperature step of 5 K and a corresponding cooling/warming rate of 5 K min^{-1} . The temperature errors are higher than those for LT-SIRM, but generally less than ± 1 K. Before running the samples, the ambient field in the measurement chamber of the magnetometer was carefully adjusted to 0.0 ± 100 nT. The effects of such a low ambient field on the measured remanence during LTD are negligible.

To further determine the mineral transformations during heating, detailed hysteresis loops were measured for the thermal products with a temperature step of 10 °C between 120 and 200 °C, and 25 °C above the 200 °C run.

Magnetic extracts for the characteristic loess sample ($L_B/34.45$ m) and its 300 °C (L_{300}) and 700 °C (L_{700}) thermal products as well as an unheated palaeosol sample ($P_B/35.89$ m) were obtained in a continuous-loop flow magnetic separator driven by a pump, using a high-gradient magnet. Mineral phases in the magnetic extracts were identified by XRD using a Siemens D5005 X-ray diffractometer with a sealed tube and monochromatic Cu- K_α radiation. The scan speed was $0.005^\circ 2\theta \text{ s}^{-1}$. Peaks of quartz (as an internal standard) were used to calibrate the raw diffractograms.

4 RESULTS

4.1 Magnetic measurements

Table 1 shows the room-temperature hysteresis parameters and susceptibility of five selected characteristic samples before and after 150 °C and 300 °C thermal treatments. Initially, the loess samples have susceptibility values between 14.8×10^{-5} SI and 16.8×10^{-5} SI, almost half the values of the palaeosols. In addition, the loess samples also have systematically higher coercivities (B_{cr} and B_c) but lower M_{rs} and M_s than palaeosols. After heating, all the hysteresis parameters and ratios decrease. Relatively speaking, the 300 °C treatment has minor effects on the magnetic properties compared with the 150 °C treatment.

The Day-plot behaviour of these five samples is illustrated in Fig. 2. The initial grain size of loess samples indicated by the Day plot is somewhat coarser than that of palaeosols. Apparently, both the loess and palaeosol data depart from the synthetic sample trend for titanomagnetite (Fig. 2) measured by Day *et al.* (1977). After heating, they simultaneously shift back to the synthetic trend along two almost parallel paths (dashed arrows in Fig. 2).

Variations in hysteretic parameters can be used to monitor the mineral transformations during heating. Fig. 3 shows that most parameters dramatically drop between 120 and 150 °C. Between 150 and 300 °C, B_c and B_{cr} further decrease but at a slower rate (Figs 3a and b). In contrast, M_{rs} increases from the minimum value at 150 °C ($\sim 3.2 \times 10^{-3} \text{ A m}^2 \text{ kg}^{-1}$) to $\sim 3.7 \times 10^{-3} \text{ A m}^2 \text{ kg}^{-1}$ at 170 °C, then remains relatively stable up to 300 °C (Fig. 3c). M_s shows a more significant increase at 170 °C with a value even slightly higher than the initial value. Similar to M_{rs} , there are no apparent changes in M_s between 200 and 300 °C (Fig. 3d). Between 300 and 550 °C, both M_{rs} and M_s steadily decrease. The changes in B_c and B_{cr} during this temperature interval are within several mT, and reach the second local minimum around 550 °C. Notable features of B_c and B_{cr} are the sharp increases above 550 °C, forming a 'U' shape between room temperature and 650 °C. On the whole B_{cr} and B_c have many of the same features for all the thermal runs.

The correlation between selected hysteretic parameters and ratios presents clearer trends after heating (Fig. 4). Generally, the variations in these hysteretic properties are classified into three stages, 25–150 °C, 160–550 °C and 550–650 °C. Between 25 and 150 °C the Day plots (Fig. 4a) gradually shift left-downward. Between 160 and 550 °C B_{cr} remains almost unchanged, but M_{rs} , M_s and B_c decrease. During the last temperature interval (550–650 °C), the points of the Day plots shift right-upward, but do not return to the initial point. Meanwhile, M_{rs} remains stable (Fig. 4b) and M_s slightly decreases (Fig. 4c). Further, B_c (Fig. 4d) gradually increases linearly after 550 °C with a slope almost identical to that between 25 and 150 °C.

In this study, sample L_B was selected to investigate the oxidation model for behaviour during heating. LT-SIRM curves for different

Table 1. Magnetic properties of representative loess and palaeosol samples and their 150 and 300 °C thermal products.

Parameter	T (°C)	L_A 33.54 m	L_B 34.45 m	L_C 36.63 m	P_A 35.19 m	P_B 35.89 m
M_{rs} ($A\ m^2\ kg^{-1}$)	25	0.0039	0.0043	0.0041	0.0061	0.0056
	150	0.0036	0.0033	0.0036	0.0051	0.0047
	300	0.0032	0.0036	0.0036	0.0051	0.0051
M_s ($A\ m^2\ kg^{-1}$)	25	0.0260	0.0275	0.0324	0.0352	0.0322
	150	0.0285	0.0233	0.030	0.0349	0.0306
	300	0.0257	0.0282	0.0298	0.0378	0.0348
B_{cr} (mT)	25	57.5	58.3	52.1	40.1	38.2
	150	34.3	43.6	34.0	24.6	32.7
	300	28.0	38.9	29.1	22.9	22.9
B_c (mT)	25	16.2	17.0	15.1	12.8	12.3
	150	11.8	13.6	11.4	9.80	11.1
	300	10.3	12.2	9.64	8.57	8.56
M_{rs}/M_s	25	0.150	0.157	0.145	0.173	0.173
	150	0.125	0.137	0.121	0.148	0.156
	300	0.125	0.127	0.12	0.136	0.147
B_{cr}/B_c	25	3.549	3.429	3.450	3.133	3.106
	150	2.907	3.201	2.982	2.510	2.946
	300	2.718	3.189	3.019	2.671	2.675
Slope ($A\ m^2\ kg^{-1}\ T^{-1}$)	25	0.0425	0.0509	0.0439	0.0486	0.0501
	150	0.0443	0.0429	0.0447	0.0461	0.0468
	300	0.0329	0.0511	0.0392	0.0418	0.0544
k (10^{-5} SI)	25	14.8	14.7	16.8	25	27.6

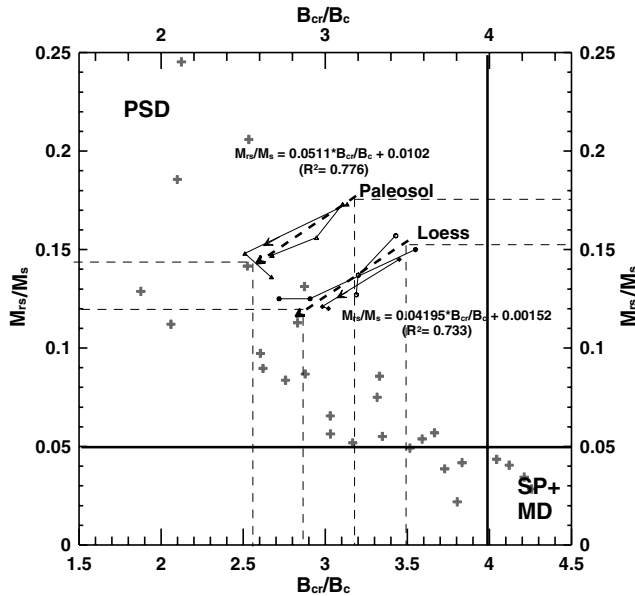


Figure 2. Day plots of the raw samples and 150 °C and 300 °C thermal products. Crosses are background information by Day *et al.* (1977). Initially, both loess and palaeosols depart from the background. After the thermal treatment, the ratios gradually shift left-downward towards the background. The equations are fitted thermal alteration trends for loess and palaeosols.

thermal products of L_B are illustrated in Fig. 5(a). To separate the sharp change due to the Verwey transition (~ 120 K) from the gradually decreasing backgrounds we used the method suggested by Liu *et al.* (2004). First, we calculate the derivative of low LT-SIRM (Fig 5b). Second, polynomial curves fitted to the data between 50 and 70 K and 150 and 300 K are subtracted from the total derivatives (Fig. 5c). The temperature-dependent maximum derivatives around the Verwey transition at ~ 120 K ($-dJ/dT_{120K}$) in Fig. 5(c) are

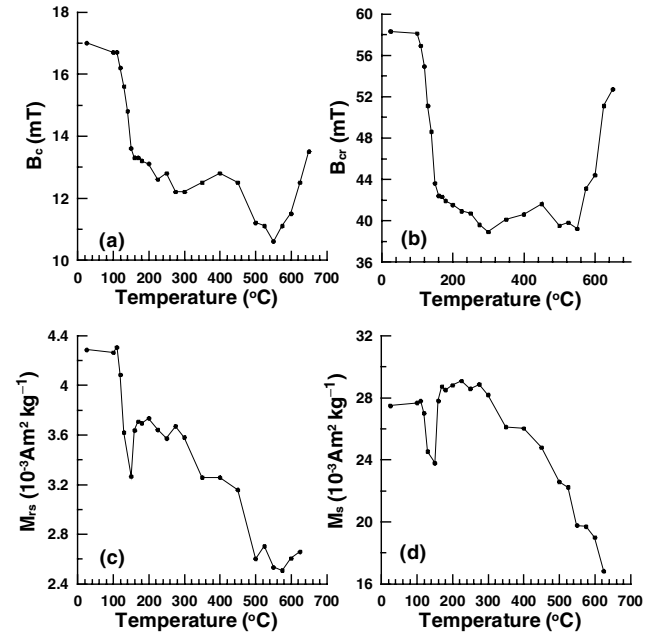


Figure 3. Variations in room-temperature hysteresis parameters for sample L_B after different thermal runs: (a) B_c , (b) B_{cr} , (c) M_{rs} and (d) M_s . Dramatic decreases in all hysteresis properties occur around 150 °C.

shown in Fig. 5(d). Unlike the coercivities, $-dJ/dT_{120K}$ does not apparently change after the 150 °C run. However, between 150 and 300 °C, $-dJ/dT_{120K}$ significantly increases by ~ 80 per cent. Above 300 °C, the normalized derivative gradually decreases to about 0.5 at 620 °C, then remains stable up to 700 °C.

Fig. 6 shows the normalized background-corrected $-dJ/dT_{120K}$. Even though the absolute maximum values of $-dJ/dT_{120K}$ for different thermal products are different, the normalized $-dJ/dT_{120K}$ for 300, 400, 500 and 600 °C runs nearly duplicate each other. All

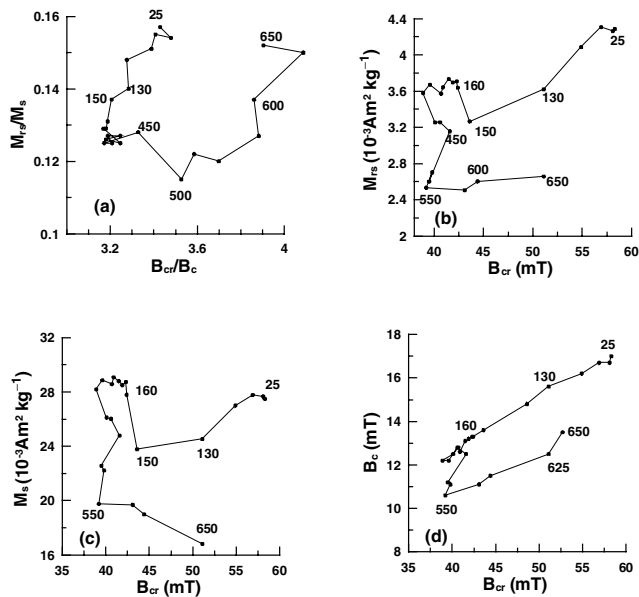


Figure 4. Bivariate plots of room-temperature hysteresis parameters and ratios: (a) Day plot, (b)–(d) M_{rs} , M_s and B_c respectively against B_{cr} . Numbers in figures are the maximum temperatures of each thermal run.

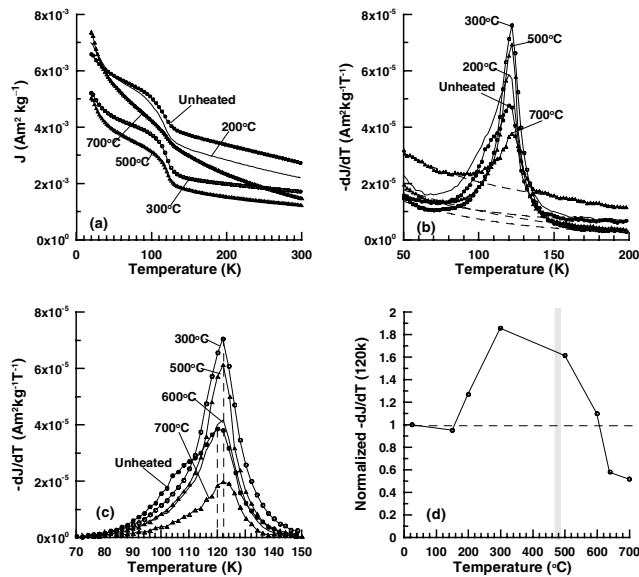


Figure 5. Low-temperature measurements for sample LB : (a) LT-SIRM, (b) first-order derivative of LT-SIRM. Dashed lines are the third-order polynomial trends fitted to the data between 50 and 70 K and 150 and 300 K avoiding the effects of Verwey transitions. (c) Background-corrected first-order derivative of LT-SIRM. (d) The maximum derivatives in (c) of the thermal products at different elevated temperatures.

of them have a 120 K peak, corresponding to the Verwey transition temperature (T_V) of stoichiometric magnetite.

Frequency-dependent susceptibility is sensitive to the SP grain concentration in the samples, especially those particles with grain size around 20 nm. Fig. 7 presents the curves for the unheated (25 °C), 600 °C and 700 °C thermal products. With increase in frequency, susceptibility gradually decreases. To calculate χ_{fd} per cent, $(k_{400} - k_{4000})/k_{400} \times 100$, where k_{400} and k_{4000} are susceptibilities at 400 and 4000 Hz respectively, linear trends were first fitted to the

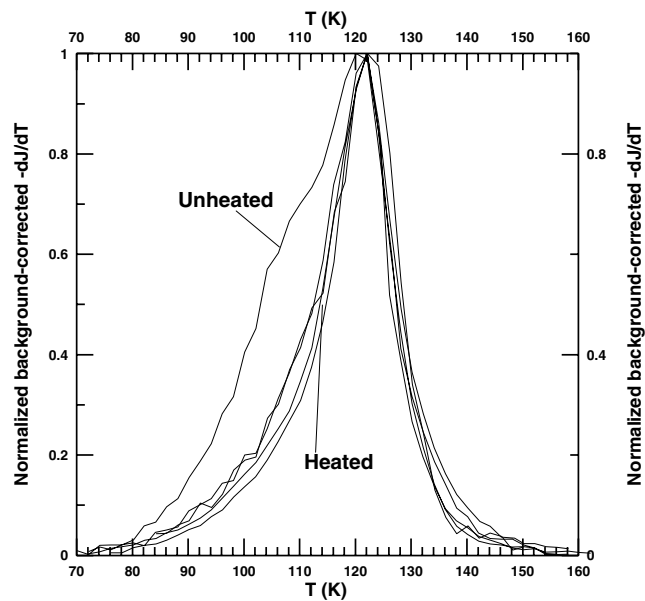


Figure 6. Normalized background-corrected derivatives of LTD-SIRM for the raw sample and 500, 600 and 700 °C thermal products. The 122 K peaks indicate the existence of stoichiometric magnetite even after high-temperature treatments.

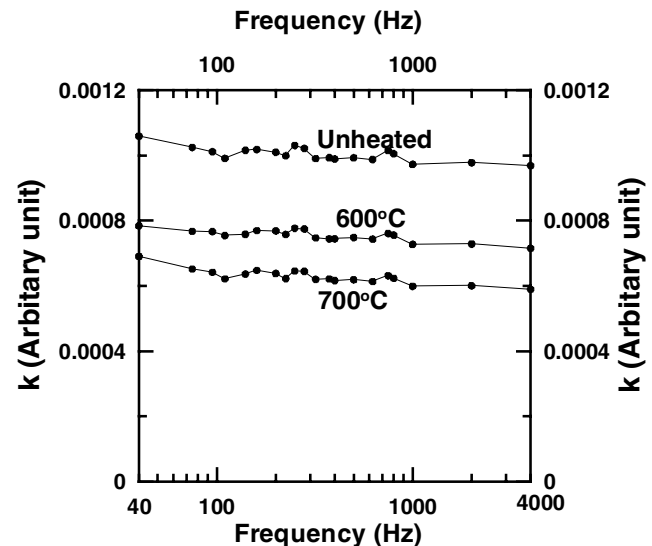


Figure 7. Variations in frequency-dependent susceptibility between 40 and 4000 Hz for the unheated, 600 and 700 °C thermal products. Clearly, with increase temperatures the magnetic susceptibility of the bulk samples gradually decreases but the slopes are visually unchanged, indicating that the absolute concentration of SP grains remains almost constant.

Table 2. Frequency-dependent susceptibility of the unheated, 600 °C and 700 °C thermal products.

T (°C)	$(k_{400} - k_{4000})/k_{400} \times 100$	$k_{400} - k_{4000}$ (10^{-5} SI)
25	5.78	5.71
600	8.15	5.94
700	10.84	6.44

data between 400 and 4000 Hz. Then k_{400} and k_{4000} are the best-fitted values. To eliminate the effects of the decrease of susceptibility after the thermal treatment we calculated the absolute value of $k_{400} - k_{4000}$. The results are summarized in Table 2. The χ_{fd} per cent values for the unheated, 600 °C and 700 °C thermal products are 5.78, 8.15 and 10.84 per cent respectively. This strongly indicates that the relative contributions of these SP grains to the bulk susceptibility potentially increase after thermal treatment. However, the slopes of these curves remain visually almost constant, and $k_{400} - k_{4000}$ is only slightly higher than its initial value (5.71×10^{-5} SI) after the 600 °C (5.94×10^{-5} SI) and 700 °C (6.44×10^{-5} SI) heating steps.

4.2 X-ray diffraction

The magnetic mineral assemblages of the concentrated magnetic extracts for the loess sample (34.45 m) and its thermal products (L_{300} and L_{700}), and the palaeosol sample (35.89 m) are characterized by XRD analysis (Fig. 8). The mineralogical identification was performed based on the data between 5 and 55° (2θ). The dominant peaks around 35.45° (hkl , 311) and 43.10° (hkl , 400) indicate the existence of magnetite. Just to the right of the magnetite peaks, two characteristic peaks at 35.63° (hkl , 311) and 43.28° (hkl , 400) are caused by maghemite. In addition, the 33.15° peak corresponds

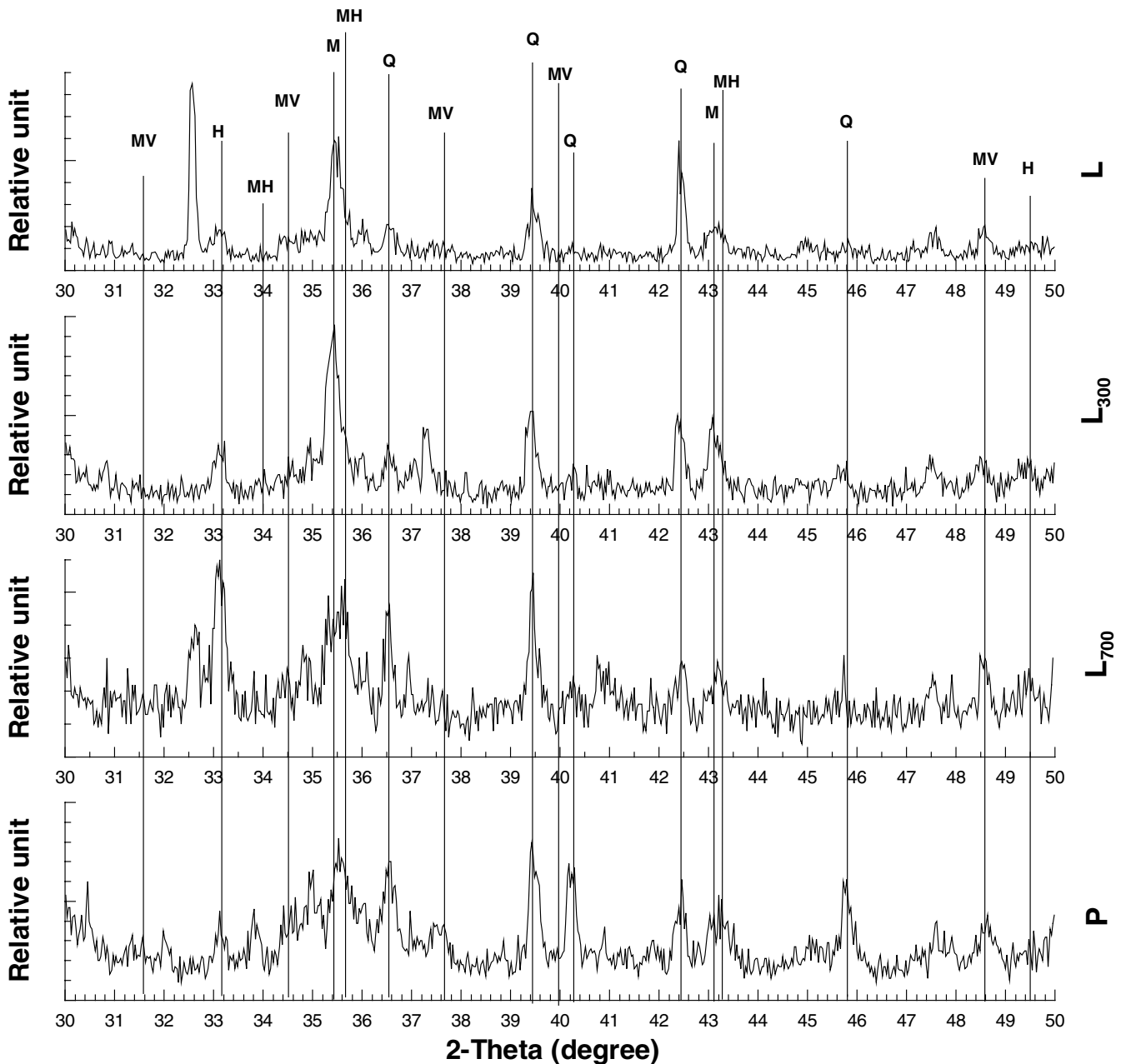


Figure 8. XRD spectrum for magnetic extracts of the loess sample (L) and its 300 (L_{300}) and 700 °C (L_{700}) thermal products and the palaeosol sample (P). The labels M, MH, MV, H and Q stand for magnetite, maghemite, muscovite, haematite and quartz respectively.

to haematite. Overall, magnetite, maghemite and haematite exist in all samples but at different relative concentrations. For the loess sample, the dominant ferrimagnetic phase is magnetite with a minor contribution from maghemite. After heating to 300 °C the highly depressed maghemite peaks and simultaneously enhanced magnetite peaks strongly indicate that some of the maghemite particles have been reduced to magnetite. With further heating up to 700 °C, the haematite peak at 33.15° is amplified and becomes comparable to the magnetite/maghemite peaks. Meanwhile, there are two subtle but distinguishable peaks at 35.45° (*hkl*, 311) and 35.63° (*hkl*, 311) with nearly equal amplitudes, indicating the coexistence of magnetite and maghemite. For the palaeosol sample, there is a maximum peak due to low-temperature oxidized magnetite between 35.45° and 35.63°, confirming that the magnetite particles in palaeosols are oxidized more than that in the loess sample (Liu *et al.* 2003a).

5 DISCUSSION

5.1 Oxidation of magnetite during heating

The loess sample L_B was selected to conduct detailed rock magnetic measurements for determining the effects of LTO on properties of the partially oxidized magnetites because of its representative characteristics (see Fig. 1 and Table 1), and also because of minor effects of pedogenesis on the initial magnetic mineralogy. Previous studies have revealed that both loess and palaeosol samples have comparable thermal behaviours except that palaeosols have an initially finer-grained distribution of magnetic minerals with a higher degree of oxidation than the loess samples (Liu *et al.* 2002, 2003a).

Kosterov (2002) found that hysteresis loops both below and above the Verwey transition for the partially oxidized synthetic magnetite sample by Wright Inc. (manufacturer 3006, 2–3 μm) are dominated by a ‘magnetite’ phase even though the sample is covered by a maghemite rim. He therefore concluded that the low-temperature oxidation occurs only superficially, leaving the inner magnetite core relatively intact. Liu *et al.* (2003a) also found stoichiometric magnetite behaviour of low-temperature measurements for palaeosol samples, in which magnetites are supposed to have been partially oxidized. They suggested that the stoichiometric magnetite behaviour is caused by the inner core, and this stoichiometric magnetite core behaves independently of the maghemite rim, especially for the low-temperature measurements.

Fig. 5(c) reveals that the amplitude of Verwey transition dramatically changes ($-dT/dT_{120K}$ increases and decreases below and above 300 °C) during heating, but the maximum of $-dJ/dT$ is fixed around 120–122 K, strongly indicating the stoichiometric magnetite behaviour. XRD results (Fig. 8) further show that magnetite does exist in the magnetic extract even after heating to 700 °C. This further supports that the inner magnetite core is always stoichiometric even though the oxidation front gradually processes down to the particle centre, resulting in a diminished (in size) inner core. This study confirms the earlier conclusion by Liu *et al.* (2003a) that there are pitfalls when estimating the degree of oxidation solely by the value of T_V for partially oxidized coarser-grained (PSD/MD) magnetite because the magnetite core of these particles remain stoichiometric even the particle has suffered a high degree of oxidation. However, combining both T_V and the amplitude of $-dJ/dT_{120K}$ can help to clarify this ambiguity (Liu *et al.* 2003a). The existence of maghemite after heating to 700 °C confirms that maghemite in the Chinese loess/palaeosols can only be partially transformed into haematite (Liu *et al.* 2003a).

5.2 Changes in magnetic properties after heating

The most striking feature of the thermal behaviour around 150 °C caused by LTO has been previously reported by van Velzen & Zijderfeld (1992, 1995), van Velzen & Dekkers (1999b) and Liu *et al.* (2002). We believe that LTO dramatically affects the magnetic properties of magnetite in the following ways. First, LTO increases the coercivity of magnetite but decreases its susceptibility (van Velzen & Zijderfeld 1992, 1995; Cui *et al.* 1994; van Velzen & Dekkers 1999b) due to the enhancement of stress caused by the difference in lattice constant between the magnetite core and the maghemite rim. Second, it depresses the amplitude of the Verwey transition, but also shifts T_V to a lower temperature (Özdemir *et al.* 1993; Honig 1995). van Velzen & Zijderfeld (1995) put forward the idea that thermal treatment (e.g. heating to 150 °C) can sharply accelerate the diffusion rate of Fe²⁺ ions from the magnetite core to the maghemite rim, thus reducing the oxidation gradient and increasing the overall degree of oxidation of the magnetite core. van Velzen & Dekkers (1999b) further proposed that such a pre-heating process (150 °C) is necessary to remove the effects of LTO. However, our current study shows that the inner magnetic cores always remain stoichiometric, although they are diminished in size. Thus we believe the diffusion of Fe²⁺ is limited to the oxidation front between the magnetite core and the maghemite shell when temperatures are between 120 and 150 °C. This is also demonstrated by a slight change in $-dJ/dT_{120K}$ after the 150 °C run, indicating that the magnetite core has not apparently been altered.

Due to release of the stress at this stage, the hysteretic parameters are restored to their ‘normal’ levels after heating to 150 °C. van Velzen & Dekkers (1999b) argued that only the hysteretic behaviour after such a 150 °C thermal treatment reflects the authentic grain size-dependent properties. The current study supports this idea that the right-upward shift in the Day-plot behaviour of the loess/palaeosol sequences is caused by LTO rather than the SP contribution as suggested by Dunlop (2002b). The positive correlation between B_{cr} and M_{rs} , especially between the 120 and 150 °C runs, strongly suggests that the loss of M_{rs} is also controlled by the release of stress instead of mineral transformations.

Between the 150 and 300 °C runs, $-dJ/dT_{120K}$ is sharply enhanced by ~85 per cent, but the normalized derivatives of background-corrected LT-SIRM for different thermal products exhibit replicated patterns (dominated uniquely by the 120 K T_V , Fig. 6). The absolute increase of $-dJ/dT_{120K}$ is caused by increase in the concentration of stoichiometric magnetites by reducing processes. This is also supported by the enhanced magnetite peaks and suppressed maghemite peaks on the XRD curves (Fig. 8).

Between 300 and 500 °C, $-dJ/dT_{120K}$ slightly decreases (Fig. 5c), inferring further oxidation of magnetites. The points in the Day plots (Fig. 4a) move toward the MD plus SP grain size region. This is probably due to the increase of effects of the original SP grains when the absolute remanences decrease by alteration from magnetite to maghemite plus haematite. This model is different from Dunlop’s model (Dunlop 2002a,b), in which increasing SP contributions move points further to the right. Above 500 °C, dramatic drops in $-dJ/dT_{120K}$ (Fig. 5c) strongly suggest that magnetites have been highly oxidized again, but still leaving stoichiometric magnetite cores. The sharp loss of $-dJ/dT_{120K}$ (Fig. 5d) around 550 °C marks the inversion temperature of most of the maghemite to haematite. However, even after 700 °C heating, maghemite and magnetite phases coexist.

Above 500 °C, the points in the Day plots begin to shift to the right-upward region, corresponding to an increase of coercivities

(Figs 3a and 3b). It seems that the high-temperature oxidation above 500 °C has some effects similar to LTO, but the latter occurs only within the surface of the magnetite and the former progresses into the deeper part of the particles, leaving a much smaller stoichiometric magnetite core than in the latter case. Alternatively, the right-upward shifts in the Day plots at this temperature interval correspond to the formation of haematite transformed from maghemite. Therefore, we deduce that the new coupling between the haematite rim and the maghemite mantle can significantly increase the inner stresses of the magnetites with a higher degree of oxidation.

In summary, the alteration of magnetic minerals in the loess sample during heating is complex. Around 150 °C the dramatic changes in magnetic properties are caused by release of stress due to diffusion of Fe²⁺ from the magnetite core to the maghemite rim. Between 150 and 300 °C, the steadily enhancement of $-dJ/dT_{120\text{ K}}$ suggests that the oxidized magnetite has been gradually reduced to stoichiometric particles, probably due to the burning of the carbon and/or hydrogen in the sample above the 150 °C run. Such organic matter is burned up after the 300 °C run, then the sample suffers oxidation again.

6 CONCLUSION

We have presented here an integrated multiparameter rock magnetic study supported by XRD data on the systematic changes in magnetic mineralogy, grain size and oxidation state of magnetic minerals in the Chinese loess/palaeosols during heating. The main conclusions are:

(1) We confirm that the initial magnetites in the Chinese loess/palaeosols have been partially oxidized at low temperature, with a stoichiometric magnetite core surrounded by a maghemite rim. During the thermal treatments, these partially oxidized magnetic particles are first reduced by the burning of the organic matter below 300 °C, and then further oxidized above that, resulting in a diminished (in size) but still stoichiometric magnetite core.

(2) The absolute number of SP particles indicated by χ_{fd} increase only by ~13 per cent for the 700 °C thermal product, which cannot account for the large increases (~88 per cent) of the corresponding χ_{fd} per cent. Therefore, we conclude that the large increase of χ_{fd} per cent is mainly due to the decrease of the bulk susceptibility rather than to the increase of the concentration of SP grains during heating. The relative effects of these finer-grained particles systematically increase when the absolute remanences of samples decreases, shifting the points in Day plots towards the MD plus SP grain size region, especially between 300 and 550 °C. The left-downward shifts of the Day plots are caused by decreasing the oxidation gradient by diffusion of Fe²⁺ from the magnetite core to the maghemite rim, but the diffusion is confined to near the oxidation front and has less effect on the stoichiometry of the magnetite core. In contrast, the right-upward shifts of the Day plots coincide with a higher degree of oxidation, indicating that the increase in oxidation gradient is probably due to the new coupling between the haematite rim and the magnetite core or the maghemite mantle.

ACKNOWLEDGMENTS

This study was supported by NSF grants nos EAR 0003421 and EAR/IF 0218384, the National Science Foundation of China (NSFC) (40221402), and NSFC 40125001. All rock magnetic measurements were measured at the Institute for Rock Magnetism (IRM), which is supported by the W. M. Keck Foundation, the Earth

Science Division of the US National Science Foundation, and the University of Minnesota. We thank E. Petrovsky and J. King for their instructive comments. This is IRM publication #0401.

REFERENCES

- An, Z., 2000. The history and variability of the East Asian paleomonsoon climate, *Quatern. Sci. Rev.*, **19**, 171–187.
- An, Z.S., Kukla, G.J., Porter, S.C. & Xiao, J., 1991. Magnetic susceptibility evidence of monsoon variation on the loess plateau of central China during the last 130 000 years, *Quatern. Res.*, **36**, 29–36.
- An, Z.S. *et al.*, 1993. Episode of strengthened summer monsoon climate of Younger Dryas age on the Loess Plateau of central China, *Quatern. Res.*, **39**, 45–54.
- Banerjee, S.K., Hunt, C.P. & Liu, X.M., 1993. Separation of local signals from the regional paleomonsoon record of the Chinese loess plateau: a rock-magnetic approach, *Geophys. Res. Lett.*, **20**, 843–846.
- Chen, F.H., Bloemendal, J., Feng, Z.D., Wang, J.M., Parker, E. & Guo, Z.T., 1999. East Asian monsoon variations during Oxygen Isotope Stage 5: evidence from the northwestern margin of the Chinese loess plateau, *Quatern. Sci. Rev.*, **18**, 1127–1135.
- Cui, Y., Verosub, K.L. & Roberts, A.P., 1994. The effect of low-temperature oxidation on large multi-domain magnetite, *Geophys. Res. Lett.*, **21**, 757–760.
- Day, R., Fuller, M. & Schmidt, V.A., 1977. Hysteresis properties of titanomagnetites: grain-size and compositional dependence, *Phys. Earth planet. Inter.*, **13**, 260–266.
- Dunlop, D., 2002a. Theory and application of the Day plot ($M_{\text{rs}}/M_{\text{s}}$ versus $H_{\text{cr}}/H_{\text{c}}$), 1, Theoretical curves and tests using titanomagnetite data, *J. geophys. Res.*, **107**, 2056, doi:10.1029/2001JB000486.
- Dunlop, D., 2002b. Theory and application of the Day plot ($M_{\text{rs}}/M_{\text{s}}$ versus $H_{\text{cr}}/H_{\text{c}}$), 2, Application to data for rocks, sediments, and soils, *J. geophys. Res.*, **107**, 2057, doi:10.1029/2001JB000487.
- Evans, M.E. & Heller, F., 2001. Magnetism of loess/paleosol sequences: recent developments, *Earth Sci. Rev.*, **54**, 129–144.
- Heller, F. & Liu, T.-S., 1982. Magnetostratigraphical dating of loess deposits in China, *Nature*, **300**, 431–433.
- Heller, F. & Liu, T.-S., 1984. Magnetism of Chinese loess deposits, *Geophys. J. R. astr. Soc.*, **77**, 125–141.
- Heller, F. & Liu, T.-S., 1986. Palaeoclimatic and sedimentary history from magnetic susceptibility of loess in China, *Geophys. Res. Lett.*, **13**, 1169–1172.
- Heller, F., Shen, C.D., Beer, J., Liu, X.M., Liu, T.S., Bronger, A., Suter, M. & Bonani, G., 1993. Quantitative estimates of pedogenic ferromagnetic mineral formation in Chinese loess and palaeomagnetic implications, *Earth planet. Sci. Lett.*, **114**, 385–390.
- Honig, J.M., 1995. Analysis of the Verwey transition in magnetite, *J. Alloys Compounds*, **22**, 24–39.
- Kosterov, A., 2002. Low-temperature magnetic hysteresis properties of partially oxidized magnetite, *Geophys. J. Int.*, **149**, 796–804.
- Kukla, G., Heller, F., Liu, X.M., Xu, T.C., Liu, T.S. & An, Z.S., 1988. Pleistocene climates in China dated by magnetic susceptibility, *Geology*, **16**, 811–814.
- Liu, Q.S., Banerjee, S.K., Zhu, R.X. & Pan, Y.X., 2002. Effects of low-temperature oxidation on the natural remanent magnetization of the Chinese loess, *Chin. Sci. Bull.*, **47**, 2100–2105.
- Liu, Q.S., Banerjee, S.K., Jackson, M.J., Chen, F.H., Pan, Y.X., & Zhu R.X., 2003a. An integrated study of the grain-size dependent magnetic mineralogy of the Chinese loess/paleosol and its environmental significance, *J. geophys. Res.*, **108**, 2437, doi:10.1029/2002JB002264.
- Liu, Q.S., Jackson, M.J., Banerjee, S.K., Zhu, R.X., Pan, Y.X. & Chen, F.H., 2003b. Determination of magnetic carriers of the characteristic remanent magnetization of Chinese loess by low-temperature demagnetization, *Earth planet. Sci. Lett.*, **216**, 175–186.
- Liu, Q.S., Banerjee, S.K., Jackson, M.J., Chen, F.H., Pan, Y.X. & Zhu, R.X., 2004. Determining the climatic boundary between the Chinese loess and

- paleosol: evidence from aeolian coarse-grained magnetite, *Geophys. J. Int.*, **156**, 267–274.
- Liu, T.S. & Ding, Z.L., 1998. Chinese loess and the paleomonsoon, *Ann. Rev. Planet. Sci.*, **26**, 111–145.
- Liu, X.M., Shaw, J., Liu, T.S., Heller, F. & Cheng, M.Y., 1993. Rock magnetic properties and paleoclimate of Chinese loess, *J. Geomag. Geoelectr.*, **45**, 117–124.
- Maher, B.A. & Thompson, R., 1992. Paleoclimatic significance of the mineral magnetic record of the Chinese loess and paleosols, *Quatern. Res.*, **37**, 155–170.
- Maher, B.A. & Thompson, R., 1995. Paleorainfall reconstructions from pedogenic magnetic susceptibility variations in the Chinese loess and paleosols, *Quatern. Res.*, **44**, 383–391.
- Maher, B.A., Thompson, R. & Zhou, L.P., 1994. Spatial and temporal reconstructions of changes in the Asian palaeomonsoon: a new mineral magnetic approach, *Earth planet. Sci. Lett.*, **125**, 461–471.
- Özdemir, Ö., Dunlop, D.J. & Moskowitz, B.M., 1993. The effect of oxidation on the Verwey transition in magnetite, *Geophys. Res. Lett.*, **20**, 1671–1674.
- Pan, Y.X., Zhu, R.X., Liu, Q.S., Guo, B., Yue, L.P. & Wu, H.N., 2002. Geomagnetic episodes of the last 1.2 Myr recorded in Chinese loess, *Geophys. Res. Lett.*, **29**, doi:10.1029/2001GL014024.
- Porter, S.C., 2001. Chinese loess record of monsoon climate during the last glacial–interglacial cycle, *Earth Sci. Rev.*, **54**, 115–128.
- Tang, Y.J., Jia, J.Y. & Xie, X.D., 2003. Records of magnetic properties in Quaternary loess and its paleoclimatic significance: a brief review, *Quatern. Int.*, **108**, 33–50.
- van Velzen, A.J. & Dekkers, M.J., 1999a. The incorporation of thermal methods in mineral magnetism of loess–paleosol sequences: a brief overview, *Chin. Sci. Bull.*, **44**, 53–63.
- van Velzen, A.J. & Dekkers, M.J., 1999b. Low-temperature oxidation of magnetite in loess–paleosol sequences: a correction of rock magnetic parameters, *Stud. Geophys. Geod.*, **43**, 357–375.
- van Velzen, A.J. & Zijderveld, J.D.A., 1992. A method to study alterations of magnetic minerals during thermal demagnetization applied to a fine-grained marine marl (Trubi formation, Sicily), *Geophys. J. Int.*, **110**, 79–90.
- van Velzen, A.J. & Zijderveld, J.D.A., 1995. Effects of weathering on single-domain magnetite in Early Pliocene marine marls, *Geophys. J. Int.*, **121**, 267–278.
- Zhou, L.P., Oldfield, F., Wintle, A.G., Robinson, S.G. & Wang, J.T., 1990. Partly pedogenic origin of magnetic variations in Chinese loess, *Nature*, **346**, 737–739.

Copyright of Geophysical Journal International is the property of Blackwell Publishing Limited and its content may not be copied or emailed to multiple sites or posted to a listserv without the copyright holder's express written permission. However, users may print, download, or email articles for individual use.